HHS Public Access

Author manuscript

*Epilepsia*. Author manuscript; available in PMC 2024 April 01.

Published in final edited form as:

*Epilepsia*. 2023 April ; 64(4): 1061–1073. doi:10.1111/epi.17470.

# HETEROZYGOUS GABA$_A$ RECEPTOR β3 SUBUNIT N110D KNOCK-IN MICE HAVE EPILEPTIC SPASMS

**Shimian Qu**[1,*], **Laurel G. Jackson**[1,4,*], **Chengwen Zhou**[1], **DingDing Shen**[1,4], **Wangzhen Shen**[1], **Gerald Nwosu**[1,4,5], **Rachel Howe**[1], **Mackenzie Caltron**[1,4], **Carson Flamm**[1], **Marshall Biven**[1], **Jing-Qiong Kang**[1,3,6,#], **Robert L. Macdonald**[1,2,3,#]

[1]Departments of Neurology, Vanderbilt University, Nashville, TN 37232.

[2]Molecular Physiology and Biophysics, Vanderbilt University, Nashville, TN 37232.

[3]Pharmacology, Vanderbilt University, Nashville, TN 37232.

[4]Program in Neuroscience, Vanderbilt University, Nashville, TN 37232.

[5]Department of Biochemistry, Cancer Biology, Neuroscience and Pharmacology, Meharry Medical College, Vanderbilt University, Nashville, TN 37232.

[6]Vanderbilt Kennedy Center of Human Development, Vanderbilt University, Nashville, TN 37232.

## Abstract

**Objective——**Infantile spasms are anis an epileptic encephalopathy of childhood, and its pathophysiology is largely unknown.We generated a heterozygous knock-in mouse with the human infantile spasms-associated *de novo* mutation *GABRB3*(c.A328G, p.N110D) to investigate its molecular mechanisms and to establish the *Gabrb3*$^{+/N110D}$ knock-in mouse as a model of infantile spasm syndrome.

**Methods——**We used electroencephalography (EEG) and video monitoring to characterize seizure types, and a suite of behavioral tests to identify neurological and behavioral impairment in *Gabrb3*$^{+/N110D}$ knock-in mice. Miniature inhibitory postsynaptic currents were recorded from layer V/VI pyramidal neurons in somatosensory cortex, and extracellular multiunit recordings from the ventral basal nucleus of the thalamus in a horizontal thalamocortical slice were used to assess spontaneous thalamocortical oscillations.

**Results——**The infantile spasms-associated human *de novo* mutation *GABRB3*(c.A328G, p.N110D) caused epileptic spasms early in development and multiple seizure types in adult

[#]***Corresponding author***: Jing-Qiong Kang, M.D., Ph.D., Vanderbilt University Medical Center, 6140 Medical Research Building III, 465 21st Ave, Nashville, TN 37232-8552, Tel: 615-936-8399, Fax: 615-322-5517. jingqiong.kang@vumc.org; Jingqiong.kang@vanderbilt.edu; Robert L. Macdonald, M.D., Ph.D., Vanderbilt University Medical Center, 6140 Medical Research Building III, 465 21st Ave, Nashville, TN 37232-8552, Tel: 615-322-5978, Fax: 615-322-5517. robert.macdonald@vumc.org.

[*]These authors contributed equally.

Author Contributions

S.Q, L.J., and R.M. contributed to the conception and design of the study. All authors contributed to the acquisition and analysis of data; S.Q., L.J., K.J.Q and R.M. contributed to drafting the text and preparing the figures.

We confirm that we have read the Journal's position on issues involved in ethical publication and affirm that this report is consistent with those guidelines.

CONFLICTS OF INTEREST

Nothing to report.

*Gabrb3*$^{+/N110D}$ knock-in mice. Signs of neurological impairment, anxiety, hyperactivity, social impairment, and deficits in spatial learning and memory were also observed. *Gabrb3*$^{+/N110D}$ mice had reduced cortical miniature inhibitory postsynaptic currents and increased duration of spontaneous oscillatory firing in the somatosensory thalamocortical circuit.

**Significance——**The *Gabrb3*$^{+/N110D}$ knock-in mouse has epileptic spasms, seizures and other neurological impairments that are consistent with infantile spasm syndrome in patients. Multiple seizure types and abnormal behaviors indicative of neurological impairment both early and late in development suggest that *Gabrb3*$^{+/N110D}$ mice can be used to study the pathophysiology of infantile spasms. Reduced cortical inhibition and increased duration of thalamocortical oscillatory firing suggest perturbations in thalamocortical circuits.

## Keywords

epilepsy; epilepsy animal models; thalamocortical circuits; epileptic encephalopathy; GABRB3; animal models; infantile spasms syndrome

## Introduction

Infantile spasm syndrome (ISS) are an epileptic encephalopathy of childhood with unknown pathophysiology. Clinical features include clusters of epileptic spasms, severe developmental delay with cognitive impairment, and often hypsarrhythmia, an interictal high amplitude, chaotic pattern seen on the electroencephalogram (EEG)[1], with age of onset between 3 and 12 months[2]. Spasms are characterized as flexor, extensor, and mixed flexor-extensor involving proximal and truncal muscles and lasting 1–2 seconds[3]. Despite early diagnosis and treatment, prognosis for ISS is poor[4], and most ISS patients develop other refractory epilepsy syndromes[5]. Neurodevelopmental delay is common in ISS (~75%), with about half of patients having cerebral palsy[5]. Other behavioral characteristics include attention deficit hyperactivity disorder, anxiety, depression, learning difficulties, and autism[6]. The majority (60–75%) of ISS cases are attributed to acquired factors[7], and the remaining (25–40%) cases are most likely genetic, primarily arising from *de novo* mutations[8].

A *de novo* mutation in the γ-aminobutyric acid receptor type A ($GABA_A$) receptor β3 subunit gene (*GABRB3)* (c.A328G, p.N110D) was found in an ISS patient[9]. $GABA_A$ receptors are pentameric, ligand-gated ion channels assembled from a panel of 19 subunits, most commonly composed of 2α, 2β, and 1γ subunits[10]. $GABA_A$ receptors mediate the majority of fast inhibitory neurotransmission, and dysfunction of these receptors is associated with several epilepsy syndromes[11]. The $GABA_A$ receptor β3 subunit is widely expressed throughout the brain and is abundant in embryonic and neonatal brains, especially in the cerebral cortex, hippocampus, and other regions involved in seizure generation[12]. The β3 subunit plays an important role in neurodevelopment[13], and mutations in *GABRB3* have been associated with childhood absence epilepsy[14] and epileptic encephalopathies including ISS and the Lennox-Gastaut syndrome [9].

The GABRB3(N110D) is a rare mutation and the N110 residue is highly conserved across $GABA_A$ receptor subunits located in the N-terminal α2 helix, a structurally conserved

region that stabilizes inter-subunit interfaces by a network of hydrogen bonds and salt bridges[15]. However, the impact of the mutation in *in vivo* is unknown. In this study, we generated the heterozygous *Gabrb3*$^{+/N110D}$ KI mouse harboring the human *de novo* *GABRB3* ISS mutation, c.A328G, p.N110D. The KI mouse recapitulated the seizures and behavioral abnormalities associated with IS due to loss of neuronal β3 subunit-mediated inhibition, making it useful for further investigation of mechanisms underlying its pathophysiology and development of new treatments for ISS.

## Methods

### Gabrb3$^{+/N110D}$ KI mice and neurobehavioral tests

The *Gabrb3*$^{+/N110D}$ mouse line was generated with a targeted G328A mutation at the endogenous *Gabrb3* locus using conventional homologous recombination in B6N embryonic stem (ES) cells (Primogenix, Inc) derived from the C57BL/6N mouse. The procedures for the KI mouse construction are the same as those for generation of the *Gabrb3*$^{+/D120N}$ mice[16] except the mutation was at G328A instead of G358A of exon 4. The procedures for all neurobehavioral tests including Elevated ZeroEZ maze, Open FieldOF and Barnes maze test as well as the concern of sex effect are detailed in Supplementary Method. The mice used for neurobehavioral tests and seizure experiments were from different cohorts.

### Behavioral observations and Vigabatrin treatment in P14-P17 mice

Mice were observed for 20 minutes at a time from P10 until weaning. Twitches or spasms were recorded. .Mice were dosed with vigabatrin (100 mg/kg, i.p.) daily, on P13-P16 and observed for 20 minutes on P14-P17. We focused on P14-P17 because we did not observe obvious spasm in pups prior to P14 in our pilot study. Mice were injected after the observation period to minimize stress-induced effects. The tails of the mice were marked with a Sharpie in a unique pattern until the animals were old enough to be genotyped. The cohorts for observation and vigabatrin treatment were separate.

### EEG electrode implantation, video-EEG recording, and analysis

Synchronized video-EEGs were recorded after electrode implantation, and video-EEG monitoring was performed with a monitoring system from Pinnacle Technology as previously described[17]. Briefly, KI and wild-type littermate mice (2 to 6-months old) were anesthetized using 2–4% isoflurane, and 5 mg/kg Ketofen (s.c.) was administered. For EEG headmount affixation, t As described in a previous study[18–20]. Four (PMID: 35840120; PMID: 27340224; PMID: 31022638), fourFour holes for holding the electrode screws were drilled through the skull to the dura mater, with two placed 3.0 to 3.5 mm anterior to the bregma and two placed 3.0 to 3.5 mm posterior to the bregma and each being 1.5 mm lateral to the central sulcus. Although the exact location varies a bit based on user placement but typically EEG 1 covers the posterior region and EEG 2 spans frontal to parietal region. The EEG 1 lead typically includes more hippocampal activity as it is closer to the posterior hippocampus while the EEG 2 lead includes more delta activity as it incorporates frontal regions. They are designed to give an overall global view of cortical activity. The EMG(electromyography) electrodes were inserted into the nuchal muscles. Following a seven-day recovery period, the mice were moved to video-EEG recording

chambers. The head mounts were connected to a pre-amplifier (#8202-SE), which connected to the 3-channel data acquisition and conditioning system (#8206-SE, Model 4100) to record from 2 EEG channels and 1 EMG channel. Video-EEG monitoring lasted for 24 h with freely moving mice in the chamber. The acquisition rate for these channels was 400 Hz. The pre-amplifier filtered at 1 Hz high pass and amplified the signal at a gain of 100X. Video-EEG-EMG data were analyzed offline with Sirenia® Seizure software (Supplementary Method). The detailed EEG analysis has been described in our previous study. Seizure events were automatically detected by the software but were manually confirmed with synchronized video monitoring to minimize detection artifact. The reviewer was blind to the genotypes.

### Whole cell slice recording

Acute brain slices were prepared according to previously published methods[21]. Coronal brain slices (300 μm) were cut from brains from 30-day-old mice using a LEICA VT-1200S vibratome (Leica Inc, Buffalo Grove, IL, USA) with oxygenated dissection solution (mM: 2.5 KCl, 0.5 $CaCl_2$, 10 $MgSO_4$, 1.25 $NaH_2PO_4$, 24 $NaHCO_3$, 11 Glucose, 214 Sucrose). The brain slices were transferred to oxygenated ACSF (mM: 126 NaCl, 2.5 KCl, 2 $CaCl_2$, 2 $MgCl_2$, 26 $NaHCO_3$, 10 Glucose, pH 7.4) and recovered at room temperature for 1 hour before experiments.

Layer V pyramidal neurons were selected for recordings and were distinguished by their large soma size with apical dendrites, and layer VI pyramidal neurons were distinguished by their position right above white matter within coronal section brain slices. Whole-cell recordings of somatosensory cortex layer V/VI pyramidal neurons were obtained according to previously published methods[21] (Supplementary method).

### Thalamocortical oscillations

Horizontal thalamocortical brain slices (350–400 μm) were prepared[22] from P30 mice and were put on top of a self-made nylon mesh interface. One unipolar tungsten electrode (MultiClamp 700B, current-clamp mode) was placed in the VBn of the thalamus to record spontaneous multi-unit activity, which was band-filtered between 100 Hz and 3 kHz. Experiments were performed at 31–32°C for 1–2 hours to collect sufficient spontaneous multi-unit activity. Data were analyzed with Clampfit (spike histogram and autocorrelation function) and Matlab to obtain auto-correlograms. Oscillation indices were calculated to compare spontaneous multi-unit activity in thalamocortical slices from wt and KI mice [23].

### Statistical analysis

Data were analyzed with GraphPad Prism 8 or the statistical package for the social sciences (SPSS) 23.0 software. Two-way ANOVA, independent-samples *t*-tests or a chi-square ($\chi^2$) test were used for the comparisons between genotypes when appropriate. Normality and equal variances were tested. For those non normally distributed data, a nonparametric Wilcoxon rank sum test was used. All analyses used an alpha level of 0.05 to determine statistical significance. Data were presented as Mean ± SEM.

## Results

### Gabrb3$^{+/N110D}$ KI pups had epileptic spasms consistent with ISS.

We generated the Gabrb3$^{+/N110D}$ KI mice by using conventional homologous recombination. The correctly targeted ES cell clones were identified by long-range PCR with one of the primers outside of the homologous arms to exclude the clones with random vector insertion (Fig. 1A). PCR fragments were digested with the Hind III (H3) enzyme to further confirm correctly targeted recombination (Fig. 1B). Chimeric mice were bred with Flpe transgenic mice to screen for germline transmission and to excise the PGK-Neo selection cassette. The leftover FRT site allowed convenient genotyping (Fig. 1C). The presence of the G358A mutation was further confirmed by PCR/sequencing. Semi-quantitative RT-PCR showed that the mutant allele did not affect *Gabrb3* gene expression as demonstrated by glyceraldehyde-3-phosphate dehydrogenase (GAPDH) as a loading control (Fig. 1D, E). The mutation was confirmed by sequencing (Fig. 1F).

We observed the gross development of the KI mice and determined whether KI mice exhibited an epilepsy phenotype by systematic home cage observation and video-EEG analyses. KI mice developed spasms as early as P14 in their home cage. Pilot study indicated that there was no obvious spasm observed in the KI pups prior to P14. The spasms were very brief and occurred in clusters (Supplemental Video), and the magnitude varied from dramatic truncal flexion and extension to subtle head drops. The wildtype littermates had minimal amounts oftwitches or spasms while the KI pups had more obvious and frequent twitches or spasms during all the observed days (Figure 1G and H, supplementary video). The KI pups also had reduced viability and reduced body weight compared with the wild-type littermates (Supplementary Fig 1). However, the *Gabrb3*$^{+/N110D}$ mice had no difference in $GABA_A$ receptor subunits $\alpha 1$, $\beta 3$, and $\gamma 2$ in the cortex, cerebellum, hippocampus, and thalamus (Supplemental Fig. 2).

### Epileptic spasms in Gabrb3$^{+/N110D}$ KI mice responded to vigabatrin.

Vigabatrin is an antiseizure medication that is commonly used to treat IS patients, and in about 56.9% of patients, it effectively controls seizures[24]. It is an irreversible inhibitor of $\gamma$-aminobutyric acid transaminase (GABA-T), thus reducing metabolism of GABA and increasing GABA levels in GABAergic synapses[25]. We tested vigabatrin in wt and KI mice to assess its efficacy to control epileptic spasms from P14 through P17 and found that the average number of spasms observed in KI mice on P15 and P16 were significantly lower in vigabatrin-treated KI mice. (Fig. 1H). Both the wildtype and the KI mice were slightly sedated during vigabatrin treatment.

### Gabrb3$^{+/N110D}$ KI mice had multiple seizure semiologies and EEG patterns consistent with IS.

We observed multiple types of spontaneous seizures in adult KI mice (Supplemental Video), but not in wild-type littermates (except for infrequent, brief, typical absence-like seizures, as is expected in C57BL6 mice)[26]. Myoclonic seizures were observed most frequently (Fig. 2A), lasting approximately 1 s. They started with a sudden, brief muscle contraction accompanied by a single high amplitude sharp spike in the EEG and EMG channels (Fig.

2B). Both atypical and typical absence seizures were observed. Atypical absence seizures were associated with sudden behavioral arrest that was not always time-locked to the spike-wave discharges at seizure onset and with diffuse, slow, irregular continuous slow spike-wave discharges (3–5 Hz) that lasted up to several minutes (Fig. 2C). During the atypical absence seizures, brief, small movements were occasionally observed. Absence seizures were rare and consisted of time-locked sudden behavioral arrest and symmetrical, high-amplitude spike-wave discharges with a frequency between 4–8 Hz and a few seconds duration (Fig. 2D). Generalized tonic-clonic seizures (GTCSs) were observed relatively rarely (Fig. 2E). GTCSs are characterized by a sudden seizure onset with the loss of consciousness, a high-amplitude high-frequency tonic phase and followed a lower frequency clonic phase characterized by myoclonic and clonic jerking. In humans, tonic seizures are characterized by unilateral or bilateral sustained contraction of one or more muscle groups, lasting for a few seconds up to a minute[27].

### Gabrb3$^{+/N110D}$ KI mice had increased sensitivity to PTZ.

PTZ is a non-competitive $GABA_A$ receptor antagonist that is widely used to provoke seizures as a method to assess CNS network excitability and seizure susceptibility[28]. KI mice and wild-type littermates (between 1–3 months old) were injected intraperitoneally with PTZ, and the latencies to onset of seizures were recorded. At a dose of 30 mg/kg, KI mice had myoclonic seizures (11 of 11 within 10 min; Fig. 2F) and generalized tonic-clonic seizures (8 of 11 within 20 min; Fig. 2G). By contrast, the wildtype mice had no myoclonic or generalized tonic-clonic seizures when dosed with 30 mg/kg of PTZ. These results indicated that mutant β3(N110D) subunits affected the level of neuronal inhibition in the brain and substantially lowered PTZ seizure threshold.

### Gabrb3$^{+/N110D}$ KI mice had abnormal interictal EEGs.

EEG background consists of low-amplitude, mixed-frequency desynchronized rhythms. Analysis of interictal EEGs from KI and wild-type littermates showed significantly higher amplitude in multiple frequency ranges for KI mice (Fig. 2H). By contrast, the wildtype littermates only had minimal absence-like spike wave discharges at baseline level and higher seizure threshold upon PTZ seizure induction. This is consistent with our previous studies on other epilepsy mouse models[19].

### Gabrb3$^{+/N110D}$ KI mice had hyperactivity, abnormal social interactions, anxiety, and cognitive impairment.

Children with IS often manifest long-term neurological impairment beyond epilepsy, including autism, cognitive impairment, and hyperactivity[29]. We performed a suite of tests to compare behavioral features of KI and littermate mice.

ISS is linked to increased risk of developing autism[32]. One of the criteria for an autism diagnosis is impaired social skills. To assess sociability of KI mice, we used the three-chamber socialization test[33]. KI mice spent substantially less time exploring novel mice (Fig. 3A), indicating decreased sociability. Given the opportunity to interact with a novel or familiar mouse, wild-type mice showed a strong preference for the novel mouse. In contrast,

KI mice did not show a significant preference for the novel mouse or the familiar mouse (Fig. 3B). These results all indicate that the KI mice had reduced sociability.

To determine if KI mice were hyperactive and anxious, we used the open field test[34]. We used a 60-min time frame to determine the activity exploration during the whole hour, but the data were binned at a 5-min interval based on the standard protocol at Vanderbilt neurobehavioral core. During the 60-minute test, the number of times KI mice reared was significantly greater than wild-type littermates (Fig. 3C), and KI mice travelled significantly farther than wild-type littermates (Fig. 3D).During open field test, mice tend to accommodate with reduced activity after initial exploration. We thus compared the time spent in the center during the first 10-min. KI mice spent less time in the center of the open field relative to wild-type littermates (Fig. 3E), suggesting increased anxiety in KI mice. In addition, KI mice spent substantially less time in the open arms of the elevated zero maze than wild-type littermates (Fig. 3F). Together, these data indicated KI mice had hyperactivity and anxiety.

To assess whether KI mice had cognitive deficits, their spatial learning and memory were assayed with the Barnes maze test[35]. The latency to find the target hole was significantly greater in the first three training days for KI mice compared to their wild-type littermates, which indicated KI mice have a learning deficit. The delayed learning was reflected by a steeper learning curve in the KI mice (Fig. 4A), although the mice caught up eventually. In addition, KI mice committed a greater number of errors by entering non-target hole zones (Fig. 4B), suggesting slower acquisition in spatial learning for KI mice. During the probe trial, the KI mice spent much less time in the target hole area compared to wild-type littermates (Fig. 4C). KI mice committed increased number of entries into the non-target holes than wild-type littermates (Fig. 4D). This suggested that KI mice had impaired spatial memory.

### $Gabrb3^{+/N110D}$ KI mice had reduced mIPSC amplitudes in somatosensory cortical layers V/VI pyramidal neurons.

We investigated whether mutant β3(N110D) subunits affected the function of inhibitory synapses in somatosensory cortical layer V/VI pyramidal neurons, which are known to participate in the thalamocortical feedback loop[36]. Whole-cell patch-clamp recordings in acute coronal slices from KI mice showed decreased $GABA_A$ receptor-mediated mIPSC amplitude (Fig. 5A to E), unchanged mIPSC frequency and decay time (data not shown). The reduced current amplitudes of mutant $GABA_A$ receptors containing β3(N110D) subunits in somatosensory cortical layer V/VI pyramidal neurons from KI mice could decrease interneuron phasic GABAergic inhibition and lower the seizure threshold by promoting neuronal hyperexcitability.

### $Gabrb3^{+/N110D}$ KI mice had increased spontaneous thalamocortical network oscillations.

The balance in the ratio of excitation to inhibition critically regulates neural network activity and brain function. Impaired inhibitory neurotransmission would disrupt the balance of excitation and inhibition and lead to disinhibition and hyperexcitability in the brain, resulting in seizures and neurobehavioral disorders[37]. Thalamocortical network oscillatory

activity was recorded in VBn in a horizontal slice that retained thalamocortical circuitry. KI mice showed prolonged and high amplitude spontaneous network oscillations compared to the very short and low amplitude spontaneous network bursts in slices from wild-type littermates (Fig. 6A to C), which indicated that mutant β3(N110D) subunits caused excessive synchronization and hyperexcitability in the thalamocortical loop, producing generalized seizures.

## Discussion

ISS is an epileptic encephalopathy that can be genetic or acquired with etiologies including structural, metabolic, and other unknown factors and is associated with seizures and multiple neuropsychiatric comorbidities and related behavioral traits[4]. Substantial progress has been made in understanding the genetic basis of IS. The Epi4K consortium studied trios by whole exome sequencing identified a *de novo* mutation, A328G, p.N110D, in *GABRB3* in a patient with IS. We generated a mouse model of IS, the heterozygous *Gabrb3*$^{+/N110D}$ KI mouse, to permit study of the effects of mutant β3(N110D) subunits *in vivo*. We demonstrated that the KI mouse successfully recapitulated seizures and behavioral phenotypes in patients with IS. Although the N110D mutation was only identified in one patient, the pathophysiology identified in the mouse could provide critical insights into other *GABRB3* mutations and IS.

### Gabrb3$^{+/N110D}$ KI mice have epileptic spasms during infancy.

Home cage observations of KI and wild-type littermates were performed on P10 to P20 mice. KI pups displayed clusters of twitches or spasms only from P14 to P17. These flexion-extension spasms (Supplemental video), typically consisting of a head drop, flexed tail and subtle limb extension or flexion with brief behavioral arrest, were similar to spasms reported in models of infantile spasms[38]. Rarely were the spasms severe enough to cause the animal to lose its posture, and while twitches were observed in wild-type and KI mice, the wild-type mice did not have any flexion-extension spasms during the observation period. This suggests that the observed twitches or spasms are specific due to the mutational effect of N110D and during a specific time window as the similar epileptic spasms were not observed in the wildtype nor adult N110D KI mice

$GABA_A$ receptors play an essential role in pruning synapses and establishing neuronal circuitry, and impaired inhibition can negatively affect the activity-dependent construction of neural circuits[39]. The β3 subunits are the predominant β subunits in embryonic and neonatal development in most parts of the brain. Expression of β3 subunits remains high during adulthood in regions associated with seizure generation, including the cortex, thalamus, hippocampus, septum, and basal forebrain[40]. In addition, the β3 subunit knockout mice have been shown to develop seizures[13]. Therefore, it is reasonable to speculate that mutant β3(N110D) subunits, impairing the function of $GABA_A$ receptors, may hamper the early formation of cortical, thalamic, and hippocampal circuitry, resulting in a hyperexcitable state that precipitates development of epileptic spasms in KI pups and a variety of seizure types later in development.

### Adult Gabrb3$^{+/N110D}$ KI mice exhibit multiple seizure types.

ISS is a disease of childhood, and while the characteristic spasms usually remit by 3 to 4 years of age, many patients develop other epilepsy syndromes such as Lennox-Gastaut syndrome. Patients with Lennox-Gastaut syndrome have multiple seizure types, the predominant ones being tonic, atonic, and atypical absence seizures. Myoclonic jerks and generalized tonic-clonic seizures have also been reported in Lennox-Gastaut syndrome patients. To assess the effects of β3(N110D) in adult mice, we conducted video-EEG monitoring to characterize seizure semiologies. Myoclonic seizures were observed most frequently, and atypical absence, absence, generalized tonic-clonic and tonic seizures were also observed. In addition to recapitulating the spasms seen in infancy, the KI mouse is a promising model to study the evolution from ISS to other seizure types.

### Gabrb3$^{+/N110D}$ KI mice display features of ISS.

$GABA_A$ receptor β3 subunits are widely expressed throughout the brain during embryonic and early postnatal stages[40] and are involved in neuronal growth and differentiation[41]. Expression decreases throughout development, but remains high in the cortex, reticular nucleus of the thalamus, hippocampus, and hypothalamus[42]. Sensory processing requires many brain regions and neural circuits, but nearly all sensory information is routed through the thalamus, particularly the VBn[43], which filters and directs information to the cortex. β3 subunits are a major component of $GABA_A$ receptors in the reticular nucleus, and thus, mutant β3 subunits could impact the function of the VBn to filter inputs to the cortex, thereby affecting somatosensory processing and function[44]. Impaired somatosensory function is common in autism, which suggests that mutant β3 subunits could cause seizures and behaviors associated with autism. Patients with IS usually suffer from a wide spectrum of behavioral phenotypes that negatively impact their social and physical health. Many IS patients have significant learning and memory deficits, social impairment, hyperactivity, and anxiety. An animal model of IS that replicates both seizures and behavioral phenotypes could be a powerful tool for use in testing new therapies. With that aim, the KI mice were tested for IS-associated behaviors.

Aberrant interictal activity is considered to be strongly associated with cognitive difficulties and neurodevelopmental regression[45], which is supported by the fact that patients with well-controlled seizures by AEDs often show reduced interictal activity and a regain of cognitive functions[46]. The interictal EEG activity of KI mice were significantly different than wild-type mice, it came as no surprise that the behavioral assessments showed significant differences. In addition to hyperactivity and increased anxiety in KI mice, we found that the KI mice had significant impairment in socialization.

Taken together, these data suggest that the KI mice have many of the behavioral traits found in patients with IS, which opens the door to further study of the effects of pharmaceutical therapies on behavioral correlates, not just seizures.

### Gabrb3$^{+/N110D}$ KI mice had impaired cortical synaptic inhibition and increased spontaneous oscillations.

Our previous *in vitro* studies indicated that mutant β3(N110D) subunits slowed the activation and accelerated the deactivation of currents from β3(N110D) subunit-containing $GABA_A$ receptors, which could lead to altered IPSCs and reduced currents and inhibition. We showed that KI mice had significantly increased sensitivity to PTZ, suggesting that mutant β3(N110D) subunits negatively affected the level of neuronal inhibition in the brain. As previously discussed, *GABRB3* is widely expressed throughout the brain during early development[40] and are involved in neuronal growth and differentiation[41]. Homozygous and heterozygous *GABRB3* KO mice have increased seizure susceptibility and EEG abnormalities[47]. As major components of $GABA_A$ receptors in the thalamic reticular nucleus and the somatosensory cortex, β3 subunits play an important role in the thalamocortical circuit. Indeed, analysis of KI mice revealed two major mechanisms that have been shown to lead to epilepsy, dysfunction of GABAergic-signaling and excessive network oscillations. In KI mice, the amplitudes of mIPSCs recorded from somatosensory cortical layer V/VI pyramidal cells in coronal brain slices were reduced about 30% with no change in frequency or decay, suggesting alteration of postsynaptic, but not presynaptic, function [48]. Consistent with the notion that excessive thalamocortical synchronization and hyperexcitability occur during seizures, we found that KI mice displayed significantly prolonged, high amplitude spontaneous thalamocortical network oscillatory activity recorded in the VBn in horizontal slices that retained some of the thalamocortical circuitry.

Many studies have examined the effects of impaired GABAergic inhibition in the thalamocortical circuitry on seizure generation[49]. The decreased amplitude of cortical mIPSCs and the increased thalamocortical oscillations suggests that this circuitry is impacted in the KI mice and that the β3(N110D) subunits affect the function of the brain by reducing inter-neuronal inhibition. Impaired thalamocortical circuitry has been implicated in the propagation of absence seizures, and increased cortical activity is involved in generalized tonic clonic seizures. The neural networks involved in tonic and myoclonic seizures are less well understood. Our model of IS offers a new opportunity to study how a mutation in the widely expressed $GABA_A$ receptor β3 subunit can cause a variety of seizure types.

### Gabrb3$^{+/N110D}$ KI mice will aid in the development of therapeutic strategies for infantile spasms.

The findings presented here identify *in vivo* functional effects of the mutant β3(N110D) subunit, including decreased mIPSC amplitude in cortical layer V/VI pyramidal neurons and increased spontaneous oscillations recorded from the thalamus. The multitude of seizure phenotypes observed in the adult KI mice and the behavioral traits suggest that the mutant β3(N110D) subunit affects the function of multiple neural circuits and brain regions, including the somatosensory thalamocortical circuit. Future studies will aim to characterize additional functional effects. The *Gabrb3$^{+/N110D}$* KI mice are a useful tool in continued study of IS pathogenesis and pathophysiology. This model will hopefully aid in the development of effective therapies by addressing the epilepsy phenotype and the concomitant encephalopathies.

## Supplementary Material

Refer to Web version on PubMed Central for supplementary material.

## Acknowledgements

The authors would like to thank Luke Taylor, B.A., who contributed to analysis of video-EEGs. We would like to thank John Allison for his technical assistance in the Vanderbilt MNL. This research was supported by NIH R01 NS51590 to RLM, R01 107424, R01 107424 S-1 to C. Z and R01 121718 to KJQ. We are grateful to Dr. Hakmook Kang for his consultation on statistics.

### Data availability

The data that support the findings of this study are available from the corresponding author upon reasonable request.

## References

1. ML Z Infantile spasms Expert opinion on pharmacotherapy 2003 2003 Nov;4.
2. JD F RAH Pathogenesis of infantile spasms: a model based on developmental desynchronization Journal of clinical neurophysiology : official publication of the American Electroencephalographic Society 2005 Jan-Feb 2005;22.
3. Kellaway P, Hrachovy RA, Frost JD, Jr., Zion T. Precise characterization and quantification of infantile spasms Ann Neurol 1979 Sep;6:214–218. [PubMed: 534418]
4. Pellock JM, Hrachovy R, Shinnar S, Baram TZ, Bettis D, Dlugos DJ, et al. Infantile spasms: a U.S. consensus report Epilepsia 2010 Oct;51:2175–2189.
5. Jeavons PM, Bower BD, Dimitrakoudi M. Long-term prognosis of 150 cases of “West syndrome” Epilepsia 1973 Jun;14:153–164. [PubMed: 4515986]
6. Iype M, Saradakutty G, Kunju PA, Mohan D, Nair MK, George B, et al. Infantile spasms: A prognostic evaluation Ann Indian Acad Neurol 2016 Apr-Jun;19:228–235. [PubMed: 27293335]
7. Osborne JPL AL, Edwards SW, Hancock E, Johnson AL, Kennedy CR, Newton RW, Verity CM, O’Callaghan FJ The underlying etiology of infantile spasms (West syndrome): information from the United Kingdom Infantile Spasms Study (UKISS) on contemporary causes and their classification. Epilepsia 2010;51:2168–2174. [PubMed: 20726878]
8. Thomas RH, Berkovic SF. The hidden genetics of epilepsy-a clinically important new paradigm Nat Rev Neurol 2014 May;10:283–292.
9. Epi KC, Epilepsy Phenome/Genome P, Allen AS, Berkovic SF, Cossette P, Delanty N, et al. De novo mutations in epileptic encephalopathies Nature 2013 Sep 12;501:217–221.
10. Farrant M, Nusser Z. Variations on an inhibitory theme: phasic and tonic activation of GABA(A) receptors Nature reviews Neuroscience 2005 Mar;6:215–229.
11. Macdonald RL, Kang JQ, Gallagher MJ. Mutations in GABAA receptor subunits associated with genetic epilepsies J Physiol 2010 Jun 1;588:1861–1869. [PubMed: 20308251]
12. Hortnagl H, Tasan RO, Wieselthaler A, Kirchmair E, Sieghart W, Sperk G. Patterns of mRNA and protein expression for 12 GABAA receptor subunits in the mouse brain Neuroscience 2013 Apr 16;236:345–372. [PubMed: 23337532]
13. Homanics GE, DeLorey TM, Firestone LL, Quinlan JJ, Handforth A, Harrison NL, et al. Mice devoid of gamma-aminobutyrate type A receptor beta3 subunit have epilepsy, cleft palate, and hypersensitive behavior Proc Natl Acad Sci U S A 1997 Apr 15;94:4143–4148. [PubMed: 9108119]
14. Tanaka M, Olsen RW, Medina MT, Schwartz E, Alonso ME, Duron RM, et al. Hyperglycosylation and reduced GABA currents of mutated GABRB3 polypeptide in remitting childhood absence epilepsy Am J Hum Genet 2008 Jun;82:1249–1261.

15. Janve VS, Hernandez CC, Verdier KM, Hu N, Macdonald RL. Epileptic encephalopathy de novo GABRB mutations impair GABAA receptor function Ann Neurol 2016 Mar 7.
16. Qu S, Catron M, Zhou C, Janve V, Shen W, Howe RK, et al. GABA Brain Commun 2020;2:fcaa028.
17. Chung WK, Shin M, Jaramillo TC, Leibel RL, LeDuc CA, Fischer SG, et al. Absence epilepsy in apathetic, a spontaneous mutant mouse lacking the h channel subunit, HCN2 Neurobiol Dis 2009 Mar;33:499–508.
18. Mermer F, Poliquin S, Zhou S, Wang X, Ding Y, Yin F, et al. Astrocytic GABA transporter 1 deficit in novel SLC6A1 variants mediated epilepsy: Connected from protein destabilization to seizures in mice and humans Neurobiol Dis 2022 Jul 14;172:105810. [PubMed: 35840120]
19. TA W, W S, X H, Z L, RL M, JQ K. Differential molecular and behavioural alterations in mouse models of GABRG2 haploinsufficiency versus dominant negative mutations associated with human epilepsy Human molecular genetics 2016 08/01/2016;25.
20. TA W, NK S, JQ K. The therapeutic effect of stiripentol in Gabrg2+/Q390X mice associated with epileptic encephalopathy Epilepsy research 2019 2019 Aug;154.
21. Huang X, Zhou C, Tian M, Kang JQ, Shen W, Verdier K, et al. Overexpressing wild-type gamma2 subunits rescued the seizure phenotype in Gabrg2(+/Q390X) Dravet syndrome mice Epilepsia 2017 Aug;58:1451–1461. [PubMed: 28586508]
22. Huguenard JR, Prince DA. Intrathalamic rhythmicity studied in vitro: nominal T-current modulation causes robust antioscillatory effects J Neurosci 1994 Sep;14:5485–5502. [PubMed: 8083749]
23. Sohal VS, Keist R, Rudolph U, Huguenard JR. Dynamic GABA(A) receptor subtype-specific modulation of the synchrony and duration of thalamic oscillations J Neurosci 2003 May 1;23:3649–3657. [PubMed: 12736336]
24. Djuric M, Kravljanac R, Tadic B, Mrlješ-Popovic N, Appleton RE. Long-term outcome in children with infantile spasms treated with vigabatrin: a cohort of 180 patients Epilepsia 2014 Dec;55:1918–1925. [PubMed: 25377998]
25. Macdonald RL, Kelly KM. Antiepileptic drug mechanisms of action Epilepsia 1995;36 Suppl 2:S2–12.
26. Letts VA, Beyer BJ, Frankel WN. Hidden in plain sight: spike-wave discharges in mouse inbred strains Genes Brain Behav 2014 Jul;13:519–526. [PubMed: 24861780]
27. Werhahn KJ, Noachtar S, Arnold S, Pfander M, Henkel A, Winkler PA, et al. Tonic seizures: their significance for lateralization and frequency in different focal epileptic syndromes Epilepsia 2000 Sep;41:1153–1161. [PubMed: 10999554]
28. Dhir A Pentylenetetrazol(PTZ) kindling model of epilepsy Curr Protoc Neurosci 2012;Chapter 9:Unit9.37.
29. Paciorkowski AR, Thio LL, Dobyns WB. Genetic and biologic classification of infantile spasms Pediatr Neurol 2011 Dec;45:355–367. [PubMed: 22114996]
30. Shiotsuki H, Yoshimi K, Shimo Y, Funayama M, Takamatsu Y, Ikeda K, et al. A rotarod test for evaluation of motor skill learning J Neurosci Methods 2010 Jun 15;189:180–185. [PubMed: 20359499]
31. Cryan JF, Mombereau C, Vassout A. The tail suspension test as a model for assessing antidepressant activity: review of pharmacological and genetic studies in mice Neurosci Biobehav Rev 2005;29:571–625.
32. Srivastava S, Sahin M. Autism spectrum disorder and epileptic encephalopathy: common causes, many questions J Neurodev Disord 2017;9:23. [PubMed: 28649286]
33. Felix-Ortiz AC, Tye KM. Amygdala inputs to the ventral hippocampus bidirectionally modulate social behavior J Neurosci 2014 Jan 08;34:586–595.
34. Kraeuter AK, Guest PC, Sarnyai Z. The Open Field Test for Measuring Locomotor Activity and Anxiety-Like Behavior Methods Mol Biol 2019;1916:99–103. [PubMed: 30535687]
35. Patil SS, Sunyer B, Höger H, Lubec G. Evaluation of spatial memory of C57BL/6J and CD1 mice in the Barnes maze, the Multiple T-maze and in the Morris water maze Behav Brain Res 2009 Mar 02;198:58–68. [PubMed: 19022298]

36. Ledergerber D, Larkum ME. Properties of layer 6 pyramidal neuron apical dendrites J Neurosci 2010 Sep 29;30:13031–13044. [PubMed: 20881121]
37. Magloczky Z, Freund TF. Impaired and repaired inhibitory circuits in the epileptic human hippocampus Trends Neurosci 2005 Jun;28:334–340. [PubMed: 15927690]
38. Dulla CG. Utilizing Animal Models of Infantile Spasms Epilepsy Curr 2018 Mar-Apr;18:107–112. [PubMed: 29670486]
39. Ben-Ari Y Excitatory actions of gaba during development: the nature of the nurture Nature reviews Neuroscience 2002 Sep;3:728–739. [PubMed: 12209121]
40. Laurie DJ, Wisden W, Seeburg PH. The distribution of thirteen GABAA receptor subunit mRNAs in the rat brain. III. Embryonic and postnatal development J Neurosci 1992 Nov;12:4151–4172. [PubMed: 1331359]
41. Herlenius E, Lagercrantz H. Development of neurotransmitter systems during critical periods Exp Neurol 2004 Nov;190 Suppl 1:S8–21.
42. Pirker S, Schwarzer C, Wieselthaler A, Sieghart W, Sperk G. GABA(A) receptors: immunocytochemical distribution of 13 subunits in the adult rat brain Neuroscience 2000;101:815–850. [PubMed: 11113332]
43. Hirata A, Aguilar J, Castro-Alamancos MA. Noradrenergic activation amplifies bottom-up and top-down signal-to-noise ratios in sensory thalamus J Neurosci 2006 Apr 19;26:4426–4436. [PubMed: 16624962]
44. DeLorey TM, Sahbaie P, Hashemi E, Li WW, Salehi A, Clark DJ. Somatosensory and sensorimotor consequences associated with the heterozygous disruption of the autism candidate gene, Gabrb3 Behav Brain Res 2011 Jan 1;216:36–45. [PubMed: 20699105]
45. Chevrie JJ, Aicardi J. Convulsive disorders in the first year of life: persistence of epileptic seizures Epilepsia 1979 Dec;20:643–649. [PubMed: 115676]
46. Stroink H, Brouwer OF, Arts WF, Geerts AT, Peters AC, van Donselaar CA. The first unprovoked, untreated seizure in childhood: a hospital based study of the accuracy of the diagnosis, rate of recurrence, and long term outcome after recurrence. Dutch study of epilepsy in childhood J Neurol Neurosurg Psychiatry 1998 May;64:595–600. [PubMed: 9598673]
47. DeLorey TM, Handforth A, Anagnostaras SG, Homanics GE, Minassian BA, Asatourian A, et al. Mice lacking the beta3 subunit of the GABAA receptor have the epilepsy phenotype and many of the behavioral characteristics of Angelman syndrome J Neurosci 1998 Oct 15;18:8505–8514. [PubMed: 9763493]
48. Choi S, Lovinger DM. Decreased frequency but not amplitude of quantal synaptic responses associated with expression of corticostriatal long-term depression J Neurosci 1997 Nov 1;17:8613–8620.
49. Avoli M A brief history on the oscillating roles of thalamus and cortex in absence seizures Epilepsia 2012 May;53:779–789. [PubMed: 22360294]

**KEY POINTS**

- *Gabrb3*$^{+/N110D}$ mice have epileptic spasms from P14-P17 and display multiple seizure types in adulthood.
- *Gabrb3*$^{+/N110D}$ mice have increased spontaneous oscillations recorded from the VBn and decreased inhibition in the cortex, indicating impaired thalamocortical circuitry.
- *Gabrb3*$^{+/N110D}$ mice have deficits in social interaction, cognitive impairment, increased anxiety, and hyperactivity.

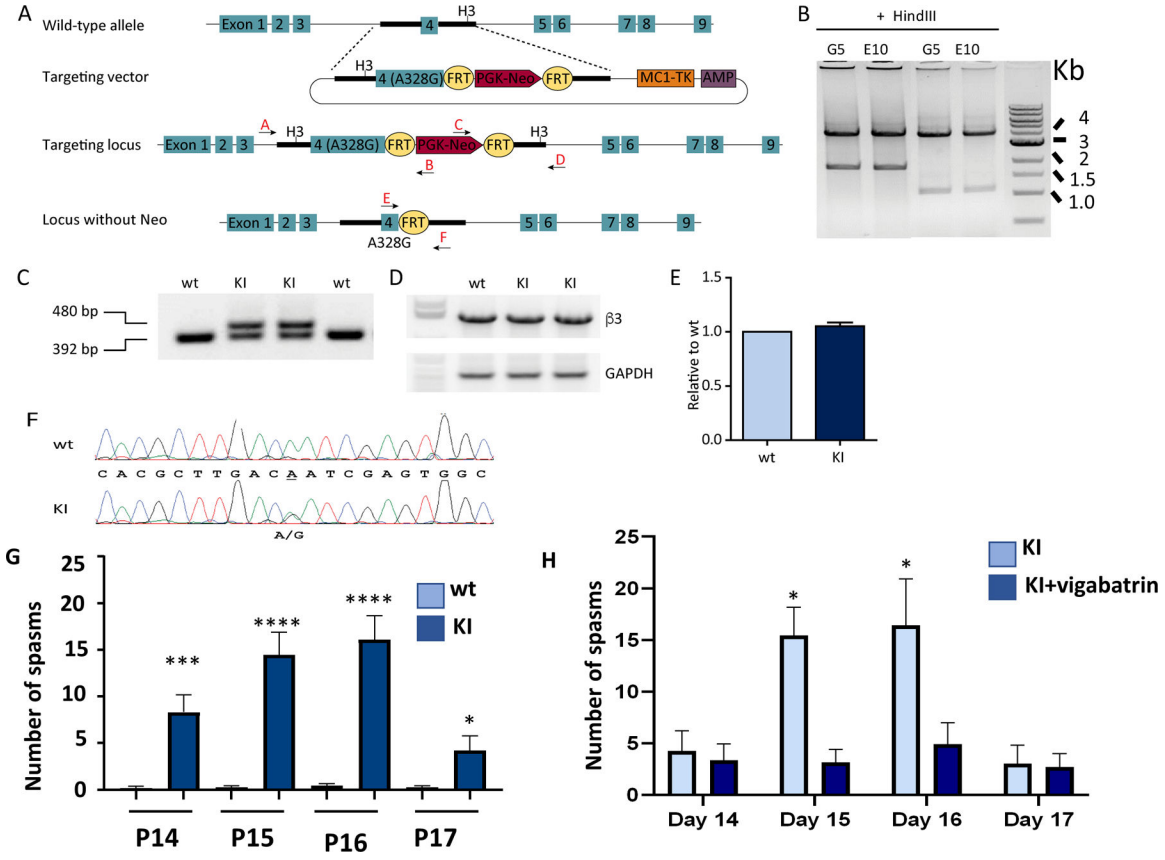


**Figure 1. Construction of the Gabrb3$^{+/N110D}$ knockin mouse model of infantile spasms**

**A.** Scheme for targeted KI of the *Gabrb3* locus. A vector was constructed to replace *Gabrb3* exon 4 genomic DNA with the positive selection cassette (PGK-Neo) and an exon 4 containing the A328G mutation. **B.** A long-range PCR strategy was used to identify the correctly targeted clones, G5 and E10. 6 kb and 4.6 kb fragments were amplified from correctly targeted clones using primers A/B and C/D, respectively. The PCR fragments were digested with the Hind III restriction enzyme (to generate the predicted 4.2 and 1.8 kb fragments for the 5' end, and 3.6 and 1 kb fragments for the 3' end) to further confirm correct homologous recombination. **C.** The KI mice were genotyped. PCR amplified a 392 bp fragment from the wild-type β3 subunit allele and a 480 bp fragment from the β3 subunit KI allele due to the insertion of FRT sequences and other modifications. **D.** Semi-quantitative RT-PCR showed that the KI allele did not affect *Gabrb3* gene expression, using glyceraldehyde-3-phosphate dehydrogenase (GAPDH) as a loading control. **E.** Band intensities of the RT-PCR products were first normalized to GAPDH for quantification, and then to wild-type levels. **F.** Sequencing chromatogram of RT-PCR derived from total brain RNA showed the presence of the G328A mutation. **G.** The number of twitches or spasms were counted in the wild-type and the heterozygous KI pups. (N=11 for both wild-type and the KI heterozygous pups). **H.** The number of twitches or spasms was counted in untreated KI pups (n = 16) and vigabatrin-treated KI pups (n = 13). In **G**, **H**, A nonparametric Wilcoxon rank sum test and A (G) Two-way ANOVA with post hoc Turkey test for multiple

comparison (H). In **G**, *P=0.0068 for P14; ****P=0.0001 for P15 and P16. In **H**, *p < 0.05 KI vs KI+vegabatrin.

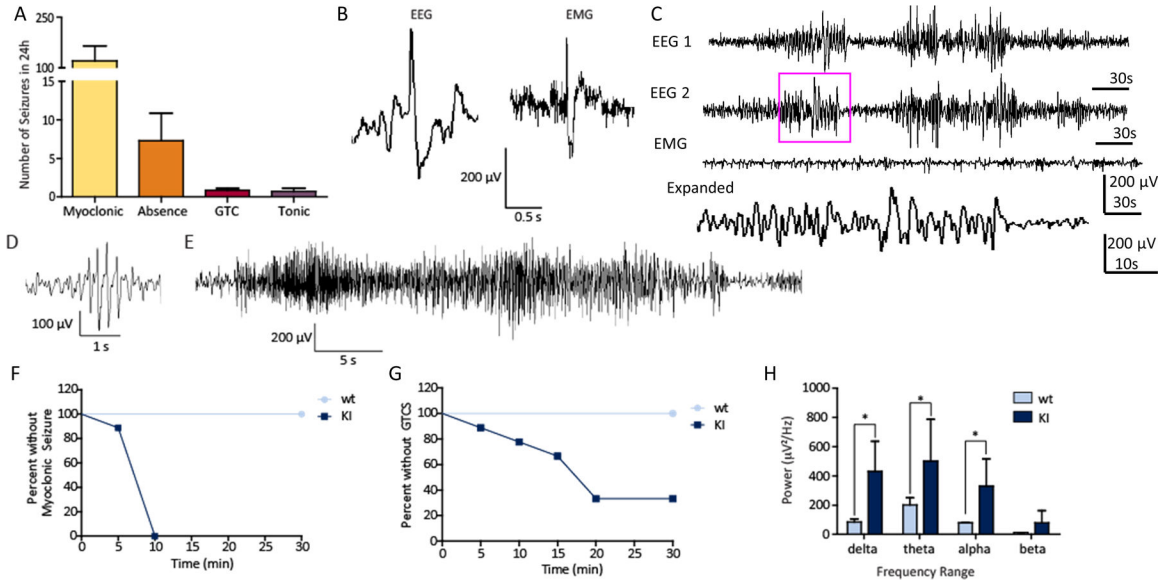


**Figure 2. Spontaneous seizures and increased PTZ sensitivity were observed in adult Gabrb3$^{+/N110D}$ KI mice.**

**A**. The average numbers of seizure that occurred in adult KI mice in a 24 h period was plotted. Myoclonic seizures were the dominant seizure type, while absence (atypical and typical) seizures were second most frequent. Generalized tonic-clonic and tonic seizures both occurred more rarely. **B-F**. Representative EEG traces for myoclonic (**B**), atypical absence (**C**), typical absence (**D**), generalized tonic-clonic (**E**) seizures were presented. In C, purple boxed segment was expanded. The traces in **B**, **D**, **E** and **F** were from channel 1. The supplementary video shows examples of each seizure type. PTZ was used to test seizure susceptibility. **F**. KI mice (11 of 11, gray line) had myoclonic seizures within 10 minutes of administration of 30 mg/kg PTZ, and 0 of 9 wt mice (black line) had myoclonic seizures (Mantel-Cox $p < 0.0001$). **G**. Generalized tonic-clonic seizures were observed in 8 of 11 KI mice (gray line) within 20 minutes of drug administration, and 0 of 9 wt mice (black line) had GTCS (Mantel-Cox $p = 0.0015$). **H**. Analysis of mean relative power of interictal EEGs showed significantly higher amplitude in multiple frequency ranges for KI ($n = 6$) compared to wt ($n = 6$) mice. Mean relative power and standard deviations were plotted for delta (0.5–3 Hz) $p = 0.022$, theta (4−-8 Hz) $p = 0.022$, alpha (8–12 Hz) $p = 0.022$. Beta (13–20 Hz) was not significantly different (Kolmogorov-Smirnov test).

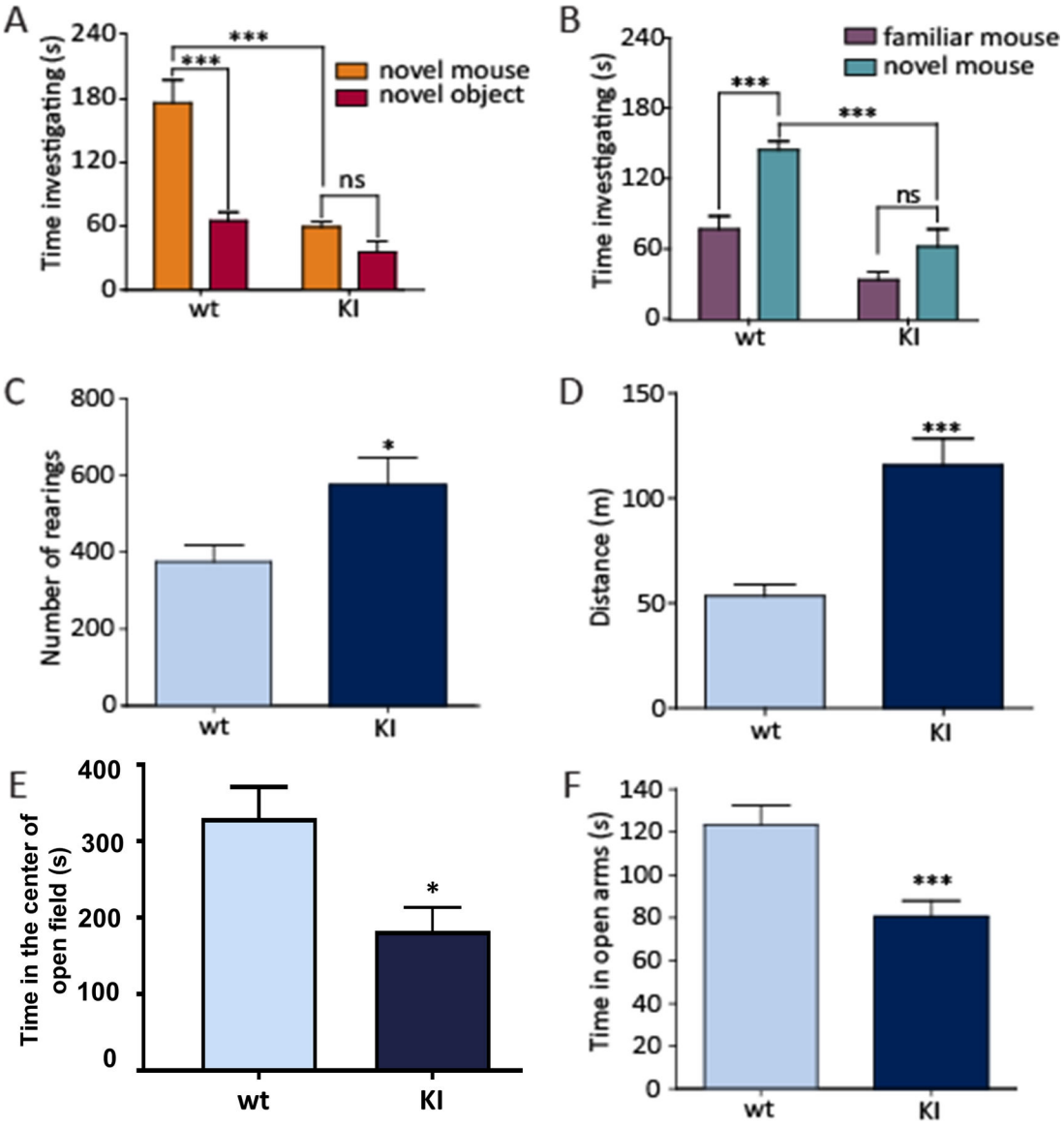


**Figure 3. Gabrb3$^{+/N110D}$ KI mice exhibited social deficits, hyperactivity, and anxiety.**

**A**, **B**. The three-chamber socialization test showed social deficits in KI mice. **A**. Sociability: KI mice spent significantly less time than wild-type mice investigating a novel mouse (Student's *t*-test, p = 0.0059). As expected, wild-type mice spent significantly more time investigating the novel mouse (Student's *t*-test, p < 0.001), and the KI mice showed no preference for the novel mouse or novel object. Two-way ANOVA showed a significant genotype effect. F(1,36)=31.61, 26.82; P<0.0001 for wt vs KI; F(1,36)=26.82, P<0.0001 for novel mouse vs novel object. **B**. Social novelty: KI mice showed no preference for a novel mouse or a familiar mouse. As anticipated, wild-type mice preferred to investigate the novel mouse instead of the familiar mouse (Student's *t*-test, p < 0.001). The KI mice spent significantly less time investigating the novel mouse compared to the wild-type mice (Student's *t*-test, p = 0.0003). Two-way ANOVA showed a significant genotype effect (p < 0.01). wt n = 9, KI n = 10. **C**, **D**. Hyperactivity was assessed using the number of open field

test for 60 mins. **C**. KI mice reared more than wt mice (wt 375.4 ± 41.48, n = 10; KI 575.4 ± 72.05, n = 9; Student's *t*-test, p = 0.0214). **D**. KI mice traveled significantly greater distances (wt 5355 ± 522.5 cm, n = 10; KI 11573 ± 1271 cm, n = 9; Student's *t*-test, p < 0.0001). **E**, **F**. KI mice displayed anxiety-like behaviors in both the open field test and the elevated zero maze. **E**. In Open Field test, KI mice spent significantly less time in the center of the open field compared to wild-type littermates during the first 10-min in the test chamber (wt 330.2.8 ± 40.76 s, n = 10; KI 182.7 ± 30.9s n = 9, unpaired two-tailed Student's *t*-test, p < 0.0115). **F**. In Elevated Zero Maze test, KI mice spent significantly less time in the open arms of the elevated zero maze (wt 123.4 ± 8.801 s, n = 10; KI 80.46 ± 7.481 s, n = 9, unpaired *t*-test, p < 0.0005).

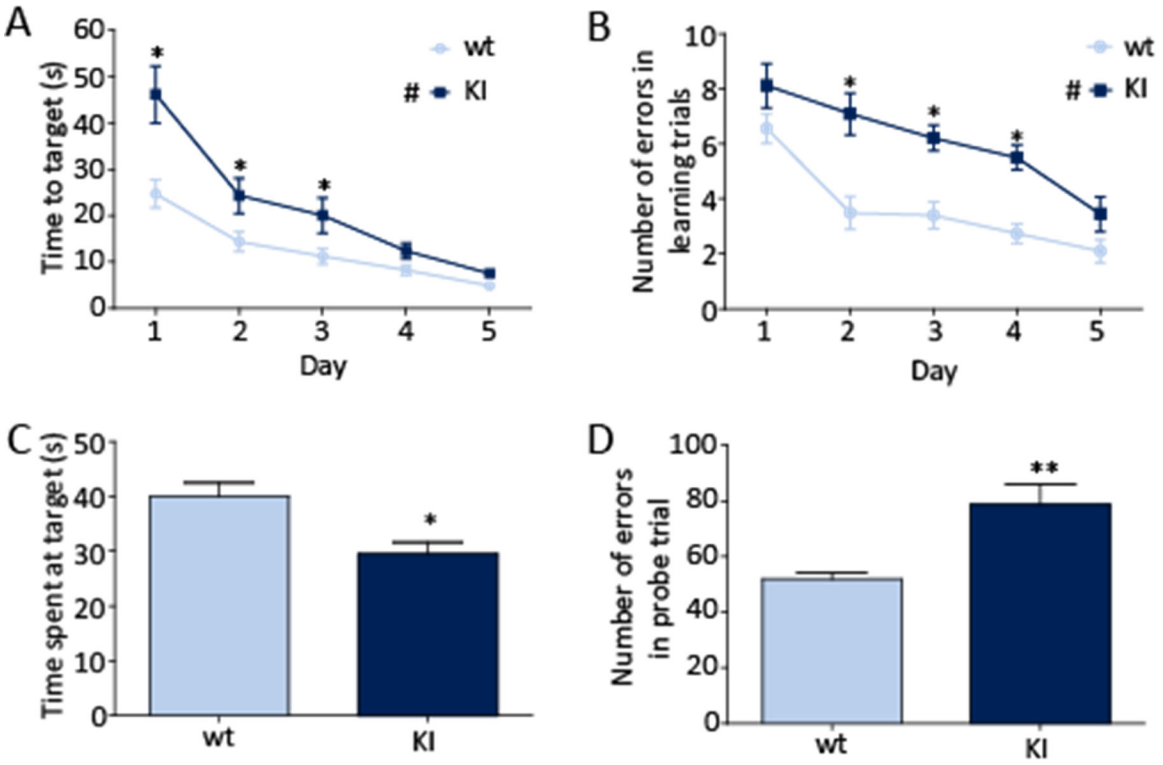


**Figure 4. Gabrb3$^{+/N110D}$ KI mice had impaired spatial learning and memory.**

Mice were tested with Barnes maze for learning and memory. Mice were pretrained on the first day of the learning trial and trained for 5 days with one trial per day before the probe trial. **A**, **B**. Five days of learning trials demonstrated a profound spatial learning deficit in KI mice. **A**. The time it took each animal (latency) to find the target hole and **B**. the number of non-target hole zones entered (errors) were quantified for each day. Two-way ANOVA for repeated measures with Bonferroni post-test, In A, F(1,14)=7.506, P<0.0160 for wt vs KI; F(4,56)=18.62, 1,098; P<0.0001 for different days. In B, F(1,70)=75.88, P<0.0001 for wt vs KI; F(4,70)=13.06, 0.5770; P<0.0001 for different days.(.wt n = 8, KI n = 8). **C**, **D**. Five-minute probe trial for spatial memory showed impaired memory in KI mice. The target hole was now covered and appeared identical to the other 11 holes. **C**. Time spent near the target hole (KI 29.46 ± 2.23 s, n = 8; wt 40.06 ± 2.45 s, n = 8) and **D**. the number of non-target hole zones entered (errors) were counted (wt 51.94 ± 2.432, n = 8; KI 78.65 ± 7.33, n = 8). Unpaired two-tailed Student's *t*-test, *p < 0.05, **p < 0.01.

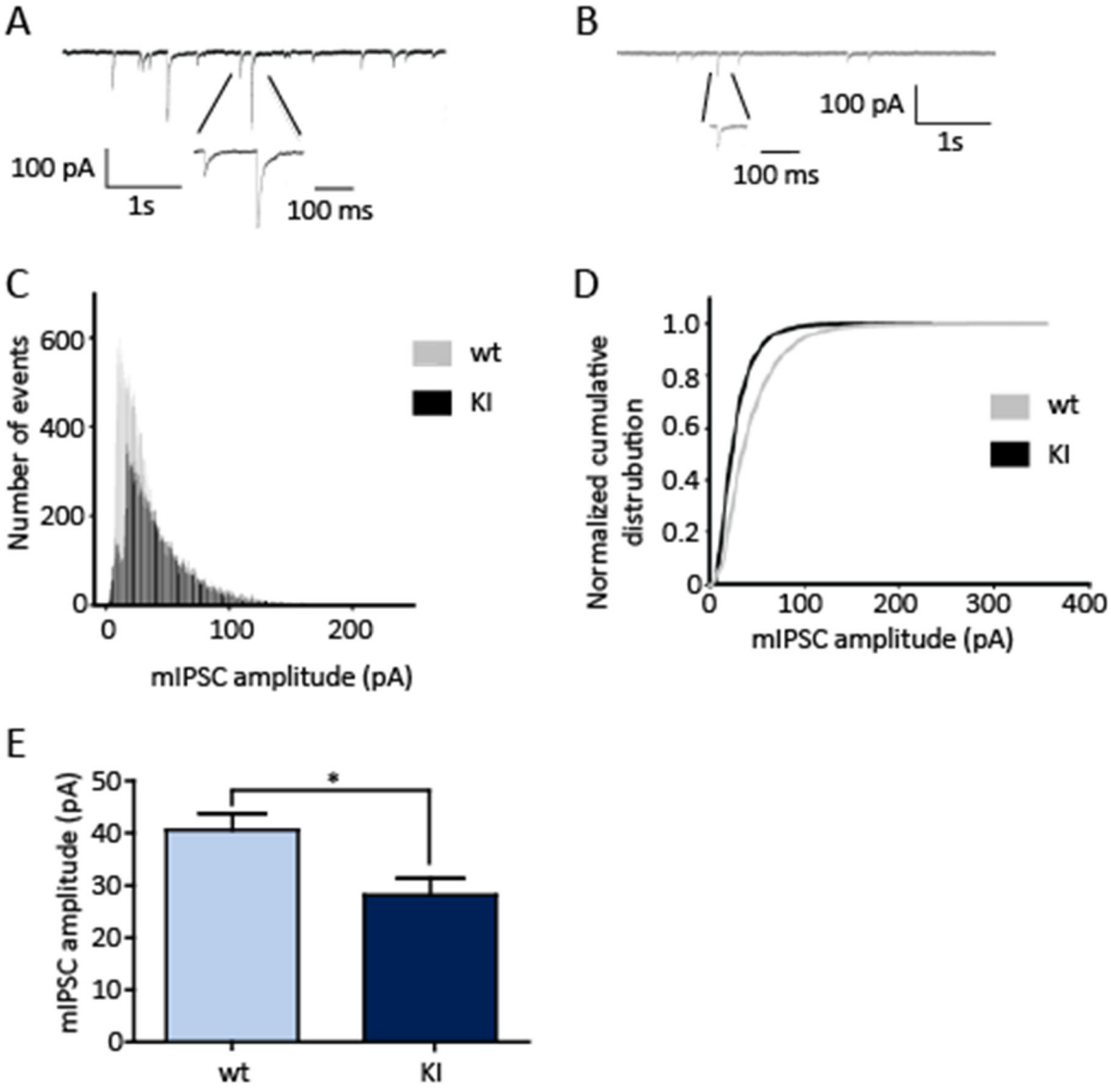


**Figure 5: Gabrb3$^{+/N110D}$ KI mice had reduced amplitude of mIPSCs.**

Representative recordings from **A**. wild-type and **B**. KI somatosensory cortical layer V/VI pyramidal neurons. **C**. Normalized mIPSC events from wild-type (gray) and KI (black) showed the frequency of mIPSCs in each amplitude bin. **D**. Normalized cumulative distribution was plotted for wild-type (gray) and KI (black) mIPSCs. **E**. Amplitude of mIPSCs from the KI mice was significantly decreased (wt 40.60 ± 3.27 pA, n = 9 neurons, 6 mice; KI 28.16 ± 3.18 pA, n = 9 neurons, 5 mice; Student's *t*-test, p = 0.014).

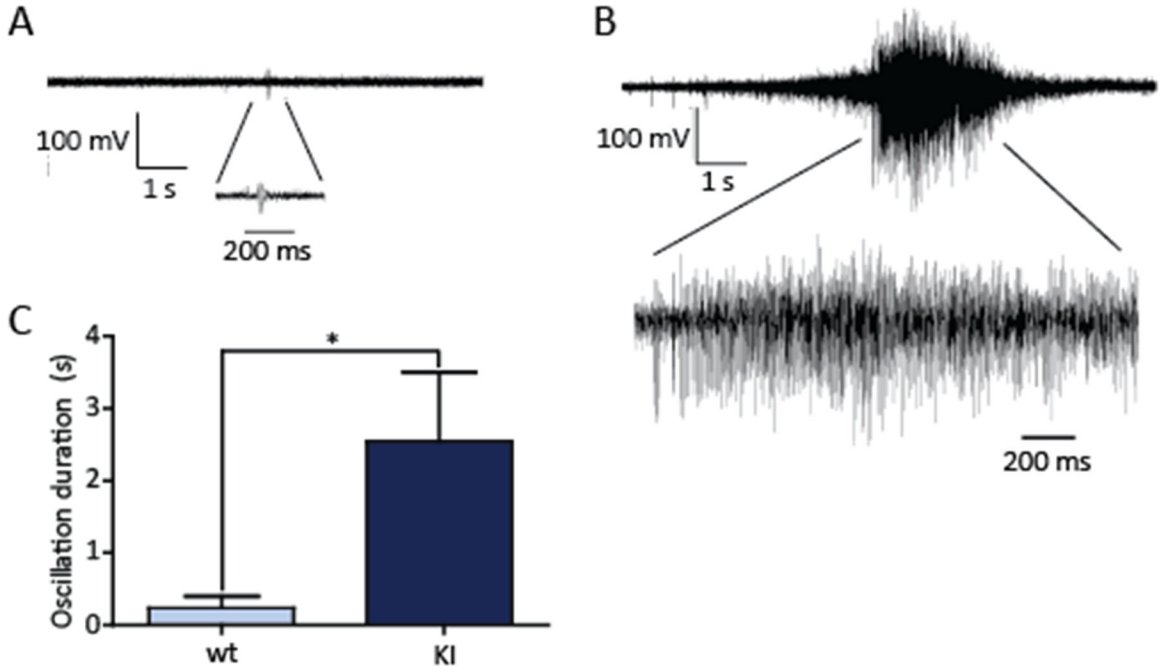


**Figure 6: Gabrb3$^{+/N110D}$ KI mice had prolonged network oscillations.**

Representative recordings from **A**. wild-type and **B**. KI horizontal brain slices showing spontaneous thalamocortical brief burst and prolonged oscillations. One short burst from a wild-type littermate mouse and one oscillation from a KI mouse were expanded to show the multiple spikes in the burst or oscillation. **C**. Average duration of spontaneous bursts from wild-type littermate mice (0.24 ± 0.16 s, 6 slices, 4 mice) and oscillations from P42 KI mice (2.55 ± 0.95 s, 6 slices, 5 mice) were plotted (Student's *t*-test, p = 0.039).